Pyridine-2-sulfonates as Versatile Ligands for the Synthesis of Novel Coordinative and Hydrogen-Bonded Supramolecules

Tarlok S. Lobana,*[a,b] Isamu Kinoshita,*[a] Kentaro Kimura,[a] Takanori Nishioka,[a] Daisuke Shiomi,[a] and Kiyoshi Isobe[a]

Keywords: Coordination polymers / Hydrogen bonds / Supramolecular chemistry / Magnetic properties / Stacking interactions

The reactions of 3-methylpyridine-2-sulfonic acid (3-mpSO$_3$H) with Cu^{II} and 4-methylpyridine-2-sulfonic acid (4-mpSO$_3$H) with Zn^{II} in water formed one-dimensional infinite coordination polymers, [Cu(3-mpSO$_3$)$_2$]$_n$ (**1**) and [Zn(4-mpSO$_3$)$_2$]$_n$ (**2**). Similarly, two-dimensional hydrogen-bonded supramolecules of stoichiometries, [ML$_2$(H$_2$O)$_2$] [L = 3-methylpyridine-2-sulfonate (3-mpSO$_3$), M = Mn (**3**), Fe (**4**), Co (**5**), Zn (**6**); L = 5-methylpyridine-2-sulfonate (5-mpSO$_3$), M = Zn (**7**); L = pyridine-2-sulfonate (PySO$_3$), M = Zn (**8**); L = 4-mpSO$_3$, M = Co (**9**)], [Ni(3-mpSO$_3$)$_2$(H$_2$O)$_2$]·H$_2$O (**10**) and the one-dimensional hydrogen-bonded network [VO(acac)(3-mpSO$_3$)(H$_2$O)] (**11**) (acac = acetylacetonate) have been prepared. The ligands are tridentate [*N*,*O*-chelating-Cu-μ-*O*-bridging] in **1** and **2**, while in all the other compounds the N,O-chelating and uncoordinated O atoms are engaged in intermolecular hydrogen bonding leading to the formation of hydrogen-bonded networks. The geometry around each metal center is octahedral (**9**) or distorted octahedral (**1**–**8**, **10** and **11**). The compounds **3**–**8**, and **10** showed novel π–π stacking interactions, not shown by **9** and **11**. The magnetic behavior of **3** and **11** indicates lack of any intermolecular magnetic interactions. The position of the substituents in the pyridyl ring and Jahn–Teller effect (Cu^{II}) appear to determine the stacking interactions as well as the density of ligands with regard to the formation of coordinative and hydrogen-bonded supramolecules.

Introduction

The hydrogen bonding and coordinative bond are the two main principles involved in the synthesis of supramolecules.[1−4] The intrinsic magnetic, optical, catalytic and structural properties of the metal ions are the prerequisites, in the field of crystal engineering, for non-linear optic, ferromagnetic, superconducting and gas-occlusion materials. The self-assembled metal complexes having one-, two-, or three-dimensional solid state networks are expected to play vital roles in the specific functions of materials.[5−8]

Pyridine-2-thione, the simplest prototype of heterocyclic thioamides, has shown its versatility in the formation of a wide range of mononuclear through to polynuclear compounds with interesting structural novelties, magnetic, electrochemical, spectral and conduction properties.[9−14] A remarkable observation is that it can bind one to four metals giving rise to polymetallic materials.[9,12] This unusual property of pyridine-2-thiolates prompted us to investigate pyridine-2-sulfonates, which are extensions of pyridine-2-thiones involving oxidation of sulfur at the 2-position of the pyridine rings. These pyridine-2-sulfonates possess one N and three O atoms (N, 3O donor set) which could provide several possibilities for coordinative and other types of bonding interactions. It may be mentioned here that only the limited coordination chemistry of pyridine-2-sulfonates is known.[15,16]

The aerobic oxidation of sulfur in 2,2′-bis(3-methylpyridine) disulfide in the presence of copper(II) bromide in methanol generated 3-methylpyridine-2-sulfonic acid, which subsequently formed an infinite one-dimensional polymer, [Cu(3-mpSO$_3$)$_2$]$_n$. A direct reaction of 3-methylpyridine-2-sulfonic acid (3-mpSO$_3$H) with Zn^{II} bromide also formed a two-dimensional hydrogen-bonded polymer, [Zn(3-mpSO$_3$)$_2$(H$_2$O)$_2$].[17] These observations stimulated our interest to systematically investigate the coordination behavior of pyridine-2-sulfonic acids. The oxidation of sulfur by the metal ions and C−S bond cleavage reactions mimic the metabolism of organic sulfur in mammals.[17,18]

In this paper, we report on novel coordination polymers and hydrogen-bonded supramolecules prepared using pyri-

[a] Department of Material Science, Graduate School of Science, Osaka City University,
Sugimoto, Sumiyoshi-ku, Osaka 558-8585, Japan
Fax: (internat.) + 81-6-6690-2753
E-mail: isamu@sci.osaka-cu.ac.jp
[b] On leave from:
Department of Chemistry, Guru Nanak Dev University, Amritsar 143005, India
Fax: (internat.) + 91-183-2-258820
E-mail: tarlokslobana@yahoo.co.in

  DOI: 10.1002/ejic.200300251

dine-2-sulfonic acid, 3-, 4- and 5-methylpyridine-2-sulfonic acids (Scheme 1) and divalent cations/oxocations, viz. VO^{2+}, Mn^{2+}, Fe^{2+}, Co^{2+}, Ni^{2+}, Cu^{2+} and Zn^{2+}. These ligands might act as multidentate ones involving *N*,*O*−chelation, *N*,*O*−chelation-Cu-μ-*O*-bridging, hydrogen bonding and π−π (pyridine ring based) interactions. All these compounds are characterized using analytical data, IR and NMR spectroscopy, X-ray crystallography and magnetic moment studies.

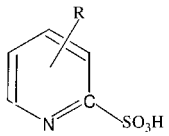

1

	Ligand
R = H	Pyridine-2-sulfonic acid ($PySO_3H$)
3-Me	3-Methylpyridine-2-sulfonic acid (3-mpSO_3H)
4-Me	4-methylpyridine-2-sulfonic acid (4-mpSO_3H)
5-Me	5-Methylpyridine-2-sulfonic acid (5-mpSO3H)

Scheme 1

Results and Discussion

Compounds **1**−**11** were prepared by the reactions of divalent cations/oxocations with neutral pyridine/substituted pyridine-2-sulfonic acids or their sodium salts. The reactions may be labeled as metathetical ones with the exchange of an anion with a metal salt by the RSO_3 anion (R = Py, x-Py, x = 3-Me, 4-Me, 5-Me) of a pyridine sulfonic acid. Allowing the reaction mixture to stand at room temperature gave crystals suitable for X-ray crystallography in many cases, while in some other cases the volume of the reaction mixture was reduced to obtain the crystals. The complexes are soluble in water as well as in alcoholic solvents such as ethanol, methanol etc. On the basis of stoichiometry, as revealed by the elemental analyses, and later confirmed by X-ray crystallography (vide infra), the complexes are grouped into four types: (a) $[ML_2]_n$ [L, M: 3-mpSO_3, Cu (**1**), 4-mpSO_3, Zn (**2**)]; (b) $[ML_2(H_2O)_2]$ [L, M: 3-mpSO_3, Mn (**3**), Fe (**4**), Co (**5**), Zn (**6**); 5-mpSO_3, Zn (**7**); $PySO_3$, Zn (**8**); 4-mpSO_3, Co (**9**)]; (c) $[Ni(3\text{-mpSO}_3)_2(H_2O)_2]\cdot H_2O$ (**10**) and (d) [VO(acac)(3-mpSO_3)(H_2O)] (**11**) (Hacac = acetylacetone). *Type a* compounds (**1**, **2**) are found to be one-dimensional covalently bonded infinite polymers, while *types b*−*d* are hydrogen-bonded (noncovalent) one- or two-dimensional (**3**−**11**) infinite polymers. Table 3 contains the crystal data and Table 1 contains bond lengths and bond angles of the compounds **1**−**11**.

The major IR spectral bands of the compounds **1**−**11** and those of the ligands are listed in the Exp. Sect. The presence of water is clearly identified by the well-defined, strong bands of the ν(O−H) and δ(O−H) stretching vibrations. The compounds **3**−**6** and **10** show three ν(O−H) peaks each, while **7**−**9** and **11** show only two such bands; however, all show one δ(O−H) stretching vibration. The splitting of the ν(O−H) peaks shows an unequivalent chemical environment in the vicinity of the O−H groups which are modulated by the hydrogen bonding; the compounds **1** and **2** show no water peaks. The peaks due to the pyridine ring are relatively strong versus those due to the methyl group. The sulfonate group RSO_3^- shows strong bands due to ν(S−O) vibrations generally found in the region 1300−1055 cm^{-1}. The ν(C−S) peak of free 3-mpSO_3H at 1035 cm^{-1} shifts to the low energy region, and were thus found in the region 1015−1031 cm^{-1}; **1** showed the largest shift.[19] Other ligands also show shifts in the ν(C−S) peaks to lower energies in their complexes. A characteristic peak due to the rocking mode of the methyl group, δ(C−CH_3) is assigned in the region 800−850 cm^{-1}. The absorption due to the vanadyl group, ν(V−O), is observed at 974 cm^{-1} as a strong peak.

Table 1−3 give a summary of important highlights of compounds **1**−**11**, bond parameters and crystal data, respectively.

Coordination Polymers

Type a compounds (**1**, **2**) belong to this category and have one-dimensional polymeric structures. The reaction of copper(II) bromide with 3-mpSO_3H in a methanol/water mixture formed monoclinic green crystals of empirical formula, Cu(3-mpSO_3)$_2$ and X-ray crystallography has shown that it exists as a one-dimensional covalently bonded polymer, $[Cu(3\text{-mpSO}_3)_2]_n$ (**1**). It is interesting to note that the aerial oxidation of 2,2′-bis(3-methylpyridine) disulfide in the presence of copper(II) bromide in methanol formed triclinic green crystals with the same crystal structure as **1**.[17] The different crystal modifications may be the consequence of the reaction conditions involved in the two cases (Table 2 and 3).

The reaction of 3-mpSO_3H with zinc(II) bromide in water did not form a polymer similar to **1**, but rather a complex with the stoichiometry, $[Zn(3\text{-mpSO}_3)_2(H_2O)_2]$ (**6**, vide infra) was formed. However, the related ligand, 4-mpSO_3H with zinc(II) bromide formed a complex of stoichiometry, Zn(4-mpSO_3)$_2$ which is also an one-dimensional coordination polymer **2**.

Figure 1 and 2 show the polymers along the *c* axis and *a* axis, respectively, with the numbering schemes (3 metal atoms shown in each case). The formation of **1** is believed to take place by initially forming the moiety, *trans*-Cu(3-mpSO_3)$_2$ (A) in which 3-mpSO_3 forms five-membered rings. This moiety (repeat unit) combines with another unit via free oxygen atoms along the axial side forming the dimer with eight-membered rings [$Cu_2O_4S_2$ core] and this process continues to finally form the one-dimensional infinite polymer. In this polymer each Cu atom is bonded to 2 N and 4 O atoms; two N and two O atoms occupy *trans* positions of the square plane of the CuN_2O_2 core and the geometry around each Cu center is elongated octahedral. The axial Cu−O [2.438(10) Å] bonds are longer than the equatorial Cu−O bonds [1.989(8) Å] by ca. 0.45 Å. Further, the equatorial Cu−O and Cu−N [1.97(10) Å] bond lengths are close to the sum of the covalent radii of Cu and O (1.93 Å) or Cu and N (1.95 Å), respectively. The longer Cu−O axial bonds lead to shorter S(1)−O(3) bonds and the free S(1)−O(2) bond length is in between the two extremes. These S−O distances are much less than the sum of the

Table 1. Bond lengths (Å) and angles (°) for compounds **1**−**11**

$[ML_2]_n$ L = 3-mpSO$_3$	$[CuL_2]_n$ (**1**) L = 4-mpSO$_3$	$[ZnL_2]_n$(**2**) L = 3-mpSO$_3$	[VOL(acac)(H$_2$O)] (**11**)	
M(1)−O(1)	1.989(8)	2.111(1)	V(1) −O(1)	2.171(2)
M(1) − O(3**)	2.438(10)	2.182(1)	V(1)−O(4), O(5)	1.974(2), 1.975(2)
M(1)−N(1)	1.97(1)	2.069(1)	V(1)−N(1)	2.155(2)
S(1)−C(1)	1.81(1)	1.790(2)	S(1)−C(1)	1.786(2)
S(1)−O(1)	1.488(8)	1.469(1)	S(1)−O(1)	1.467(2)
S(1)−O(2)	1.449(10)	1.433(1)	V(1)−O(6)	1.588(2)
S(1)−O(3)	1.409(10)	1.462(1)	V(1)−O(7)	2.060(2)
N(1)−M(1) −N(1*)	180.0	180.0	N(1)−V(1) −O(1)	76.04(6)
O(1)−M(1) −O(1*)	180.0	180.0	O(1)−V(1) −O(6)	169.59(8)
O(1)−M(1) −N(1)	86.1(4)	82.85(5)	O(4) −V (1) −O(5)	89.75(7)
M(1)−O(1) −S(1)	118.4(5)	117.74(6)	V(1) −O(1) −S(1)	123.13(9)
O(1)−S(1) −C(1)	101.8(5)	104.46(7)	O(1) −S(1) −C(1)	103.13(10)
S(1) −C(1) −N(1)	115.3(9)	116.3(1)	S(1) −C(1) −N(1)	113.7(1)
C(1) −N(1) −M(1)	116.7(8)	117.2(1)	C(1) −N(1)−V(1)	121.8(1)
			O(7) −V(1) −O(4)	91.08(8)
Intermolecular parameters				
			O(3) ··· O(7)	2.697(3)
			O(2) ··· O(7)	2.730(3)

$[ML_2(H_2O)_2]$ L = 3-mpSO$_3$	$[MnL_2(H_2O)_2]$ (**3**)	$[FeL_2(H_2O)_2]$ (**4**)	$[CoL_2(H_2O)_2]$ (**5**)	$[ZnL_2(H_2O)_2]$ (**6**)
M(1)−O(1)	2.187(2)	2.137(2)	2.103(2)	2.155(1)
M(1)−O(4)	2.164(2)	2.109(2)	2.090(2)	2.095(1)
M(1)−N(1)	2.242(2)	2.175(2)	2.126(2)	2.109(1)
S(1)−C(1)	1.802(2)	1.796(2)	1.797(2)	1.797(2)
S(1)−O(1)	1.457(2)	1.459(2)	1.463(2)	1.458(1)
S(1)−O(2)	1.443(2)	1.444(2)	1.442(2)	1.443(2)
S(1)−O(3)	1.451(2)	1.446(2)	1.444(2)	1.447(1)
N(1)−M(1)−N(1*)	155.01(9)	157.1(1)	159.8(1)	158.12(8)
O(1)−M(1)−O(1*)	96.9(1)	96.5(1)	98.1(1)	97.76(9)
O(1)−M(1)−N(1)	76.28(6)	77.99(7)	80.0(7)	79.90(5)
O(4)−M(1)−O(4*)	82.8(2)	82.3(1)	83.7(1)	83.51(9)
M(1)−O(1)−S(1)	123.75(10)	123.0(1)	121.75(10)	120.37(7)
O(1)−S(1)−C(1)	104.8(1)	104.3(1)	104.4(1)	104.82(8)
S(1)−C(1)−N(1)	114.2(1)	114.1(1)	114.1(2)	114.6(1)
C(1)−N(1)−M(1)	120.5(1)	120.2(1)	119.4(1)	120.0(1)
Intermolecular parameters				
O(2) ··· O(4)	2.814(3)	2.812(3)	2.837(3)	2.818(2)
O(3) ··· O(4)	2.718(3)	2.718(3)	2.729(3)	2.723(2)
Stacking interaction	ca. 3.47	ca. 3.48	ca. 3.49	ca. 3.50

$[ML_2(H_2O)_2]$	$[ZnL_2(H_2O)_2]$ (**7**) L = 5-mpSO$_3$	$[ZnL_2(H_2O)_2]$ (**8**) L = PySO$_3$	$[CoL_2(H_2O)_2]$ (**9**) L = 4-mpSO$_3$	$[NiL_2(H_2O)_2]\cdot H_2O$ (**10**) L = 3-mpSO$_3$
M(1)−O(1)	2.189(2)	2.156(3)	2.118(1)	2.057(2)
M(1)−O(4)	2.073(2)	2.051(3)	2.071(2)	2.057(2)
M(1)−N(1)	2.102(2)	2.144(3)	2.120(2)	2.085(2)
S(1)−C(1)	1.787(2)	1.783(3)	1.785(2)	1.795(3)
S(1)−O(1)	1.454(2)	1.453(3)	1.466(1)	1.466(2)
S(1)−O(2)	1.448(2)	1.440(3)	1.448(2)	1.440(2)
S(1)−O(3)	1.442(2)	1.438(3)	1.447(2)	1.444(3)
N(1)−M(1)−N(1*)	161.07(9)	165.2(2)	180.0	169.6(1)
O(1)−M(1)−O(1*)	98.18(10)	93.0(2)	180.0	94.3(1)
O(1)−M(1)−N(1)	80.16(6)	80.7(1)	81.37(5)	82.27(8)
O(4)−M(1)−O(4*)	85.66(10)	86.1(2)	180.0	86.6(1)
M(1)−O(1)−S(1)	117.62(9)	118.6(1)	116.98(8)	120.1(1)
O(1)−S(1)−C(1)	104.29(9)	105.3(2)	103.85(8)	104.9(1)
S(1)−C(1)−N(1)	115.3(1)	116.0(2)	114.4(1)	114.0(2)
C(1)−N(1)−M(1)	118.8(1)	117.2(2)	116.7(1)	118.4(2)
Intermolecular parameters				
O(2) ··· O(4)	2.760(2)	2.730(4)	2.769(2)	2.715(3)
O(3) ··· O(4)	2.748(2)	2.704(4)	2.741(2)	–
O(3) ··· O(5)	–	–	–	2.784(3)
O(4) ··· O(5)	–	–	–	2.760(4)
Stacking interaction	ca. 3.96	ca. 3.70	–	ca. 3.82

covalent radii of S and O atoms (1.75 Å).[20] It shows partial double bond character of the S−O bonds. The S(1)−C(1) distance is close to that of a single covalent bond length (1.79 Å) (Table 1).

The formation of polymer **2** can be viewed in a manner similar to that of **1**; however the axial Zn−O [2.182(1) Å] and equatorial Zn−O [2.111(1) Å] bond lengths are comparable and coupled with the bond angles, the geometry around each zinc(II) center is close to an ideal octahedron. It may be noted that the variations in coordinated bond lengths are controlled by the metal-oxygen interactions. The stronger M−O bonds lead to long S−O bonds and vice

Table 2. A summary of important highlights of compounds **1**−**11**

Compound	Structure type	Crystal system	Space group	π−π (Å)
$[\{Cu(3\text{-}mpSO_3)_2\}_n]$ (**1**)	Coordination polymer	monoclinic	$P2_1/n$(no. 14)	Nil
$[\{Zn(4\text{-}mpSO_3)_2\}_n]$ (**2**)	Coordination polymer	monoclinic	$P2_1/c$(no. 14)	Nil
$Mn(3\text{-}mpSO_3)_2(H_2O)_2]$ (**3**)	H-bonded polymer	monoclinic	$C2/c$(no. 15)	3.47
$Fe(3\text{-}mpSO_3)_2(H_2O)_2]$ (**4**)	H-bonded polymer	monoclinic	$C2/c$(no. 15)	3.48
$Co(3\text{-}mpSO_3)_2(H_2O)_2]$ (**5**)	H-bonded polymer	monoclinic	$C2/c$(no. 15)	3.49
$Zn(3\text{-}mpSO_3)_2(H_2O)_2]$ (**6**)	H-bonded polymer	monoclinic	$C2/c$(no. 15)	3.50
$[Zn(5\text{-}mpSO_3)_2(H_2O)_2]$ (**7**)	H-bonded polymer	monoclinic	$C2/c$(no. 15)	3.96
$[Zn(PySO_3)_2(H_2O)_2]$ (**8**)	H-bonded polymer	monoclinic	$C2/c$(no. 15)	3.70
$[Co(4\text{-}mpSO_3)_2(H_2O)_2]$ (**9**)	H-bonded polymer	triclinic	$P\bar{1}$(no. 2)	Nil
$[Ni(3\text{-}mpSO_3)_2(H_2O)_2]H_2O$ (**10**	H-bonded polymer	monoclinic	$C2/c$(no. 15)	3.82
$[VO(3\text{-}mpSO_3)(acac)(H_2O)]$ (**11**)	H-bonded polymer	monoclinic	$P2_1/c$(no. 14)	Nil

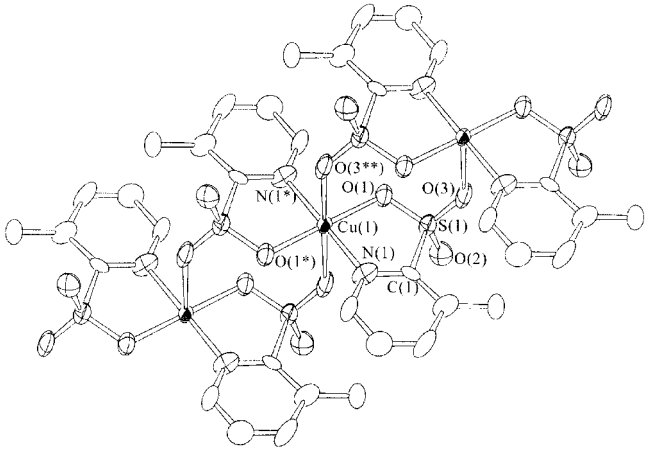

Figure 1. One-dimensional infinite structure of $[\{Cu(3\text{-}mpSO_3)_2\}_n]$ (**1**) along the *c* axis

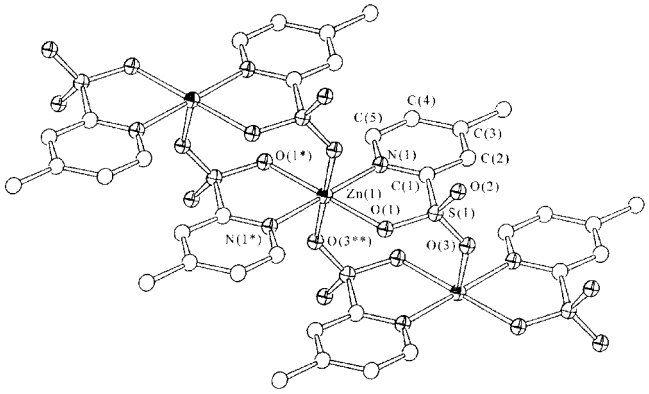

Figure 2. One-dimensional infinite structure of $[Zn(4\text{-}mpSO_3)_2]_n$ (**2**) along the *a* axis

versa. The S(1)−O(2) bonds of the RSO_3 groups, which are not involved in bonding to the metals in polymers **1** and **2** are also marginally affected by the change of the metal (Table 1). The OMN bite angle is 86.1(4)° in the Cu polymer and 82.85(5)° in the zinc polymer and this is probably linked with the size of the metal center. The angles at O(1), S(1), C(1) and N(1) are also affected by the bite angles. The large bite angle at the Cu^{I} center is accompanied by a relatively large angle at O(1) and smaller angles at S(1), C(1), and N(1), while the reverse trend is shown by the zinc polymer. Thus in compounds **1** and **2**, $3\text{-}mpSO_3^-$ and $4\text{-}mpSO_3^-$ ligands act as N,O,O donor sets with one free S−O bond in each case.

Structures of Mononuclear Units (*Types b*−*d*)

Compounds **3**−**9** (*type b*) have the same structural formula, $[ML_2(H_2O)_2]$ and the differences lie in the nature of the metal, presence of a methyl substituent in the pyridyl ring and the position of the water ligands. Thus the compounds, **3**−**6** have $3\text{-}mpSO_3^-$ while **7**−**9** have $5\text{-}mpSO_3^-$, $PySO_3^-$ and $4\text{-}mpSO_3^-$, respectively, as the anionic ligands. Further, H_2O molecules occupy *cis* positions of the octahedral compounds **3**−**8** (Figure 3) and *trans* positions in compound **9** (Figure 4).

Compounds **3**−**8** are monoclinic with space groups, $C2/c$, **9** has triclinic crystals with space group $P\bar{1}$, and **3**−**6** are isomorphic. It shows that the position of water in the octahedron and not the substituent of the pyridyl ring most probably determines the crystal system (Table 2 and 3). Figure 3 (only structure of compound **3** shown) and Figure 4 (compound **9**) show the numbering schemes of the complexes. The molecular structure of each of compounds **3**−**9** consists of two N,O-chelating RSO_3^- (R = Py, x-Py) ligands and two water molecules; the divalent metal center, Co^{II} is located on the crystallographic inversion center in compound **9**.

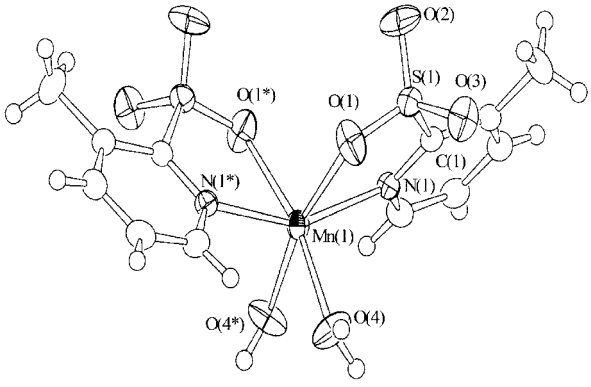

Figure 3. ORTEP drawing of $[Mn(3\text{-}mpSO_3)_2(H_2O)_2]$ (**3**) showing the numbering scheme

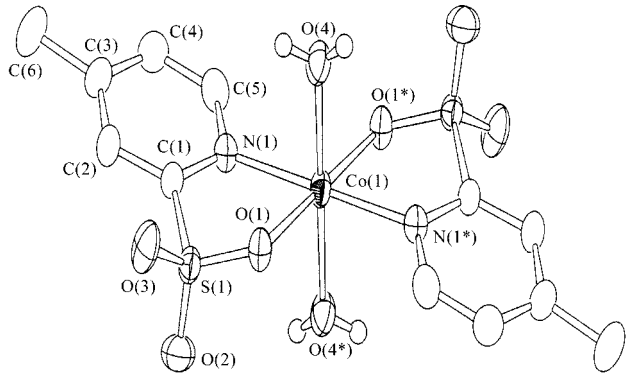

Figure 4. ORTEP view of *trans*-[Co(4-mpSO$_3$)(H$_2$O)$_2$] (**9**) showing the numbering scheme

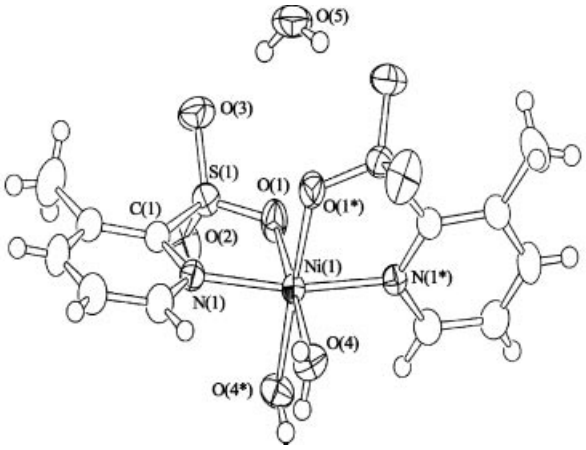

Figure 5. ORTEP view of *cis*-[Ni(3-mpSO$_3$)$_2$(H$_2$O)$_2$]·H$_2$O (**10**)

A discussion on the differences in the bond parameters of **3**−**9** now follows. In these compounds, M(1)−O(1), O(1*), N(1) and N(1*) bonds are related to the RSO$_3^-$ moiety and M−O(4), O(4*) bonds refer to the coordinated H$_2$O molecules. The oxygen atoms of S−O(2) and S−O(3) bonds are free and engage in the intermolecular hydrogen bonding (vide infra). In compound **3**, the M(1)−O(1) bond length, 2.187(2) Å, is close to the sum of the covalent radii of Mn and O (2.12 Å).[20] The Mn(1)−O(4) bond length, 2.164(2) Å, is less than the Mn(1)−O(1) bond length and it shows that water is relatively more tightly bonded to Mn(1). The Mn(1)−N(1) bond length, 2.242(2) Å, is also close to the sum of the covalent radii of Mn and N (2.14 Å).[20] The trend in M(1)−O(1), O(4), N(1) bond lengths for compounds **4**−**9** is similar. The metal−ligand bond lengths clearly vary with the size of the central metal atom: Mn > Fe > Co > Ni. The coordinated S(1)−O(1) bond is only marginally longer than the uncoordinated S(1)−O(2), O(3) bonds in all these compounds (Table 1). All these S−O bond lengths are less than the sum of the covalent radii of S and O atoms (1.75Å).[20] Finally, S(1)−C(1) distances lie in the narrow range ca.1.783−1.802 Å and close to the single covalent bond length (1.79 Å).

Each of compounds **3**−**8** have a distorted octahedral geometry and the *trans* N(1)−M−N(1*) bond angles are in the range, ca. 155−165°; however, compound **9** has a perfect octahedral geometry. The bite angle, O(1)−M(1)−N(1) of the pyridine-2-sulfonates lie in the range, ca. 76−81° in compounds **3**−**9** and these bite angles are less than those shown by **1** (ca. 86°) and **2** (ca. 83°). Thus compound **1** showed the largest bite angle among complexes **1**−**9**. The coordinated H$_2$O molecules are *trans* in compound **9** and cause the O(4)−M−O(4*) bond angles to be ca. 82−86° in complexes **3**−**8**. The trend of bond angles at O(1), S(1), C(1) and N(1) atoms is similar to that observed in compounds **1** and **2** (Table 1).

Figure 5 and 6 show molecular structures with numbering schemes of compounds **10** (*type c*) and **11** (*type d*), respectively. Compound **10** has two chelating 3-mpSO$_3^-$ ligands, two coordinated water molecules and one lattice water molecule. It also crystallizes in the *C*-centered monoclinic space group *C*2/*c* (Table 2 and 3) and it has a molecular structure similar to that of **3** (Figure 3). The bond parameters are also similar to those of compounds 3−9 except that Ni(1)−O(1) and Ni(1)−(4) (coordinated H$_2$O) have the same bond lengths. Finally compound **11** formed monoclinic crystals with space group, $P2_1/c$ and in this compound the VO^{2+} ion is coordinated by a water molecule and two different chelating ligands, acac$^-$ and 3-mpSO$_3^-$(Table 3). The geometry around the vanadium(IV) center is distorted octahedral. The equatorial plane of the vanadyl is occupied by the O atom of the water molecule, N atom of 3-mpSO$_3^-$ and two O atoms of acac. One oxygen atom of 3-mpSO$_3$ occupies a position *trans* to the V=O group. The bond angles and lengths show trends similar to those of compounds **3**−**10**; the V=O bond as expected, is the shortest bond [V(1)−O(6) = 1.588(2) Å]. The acac$^-$ ion forms bonds stronger than those formed by the oxygen atom of 3-mpSO$_3^-$ or it may be the *trans* effect of V=O bond which lengthens V(1)−O(1) bond vis-à-vis V(1)−O(4), O(5) bonds which are short.

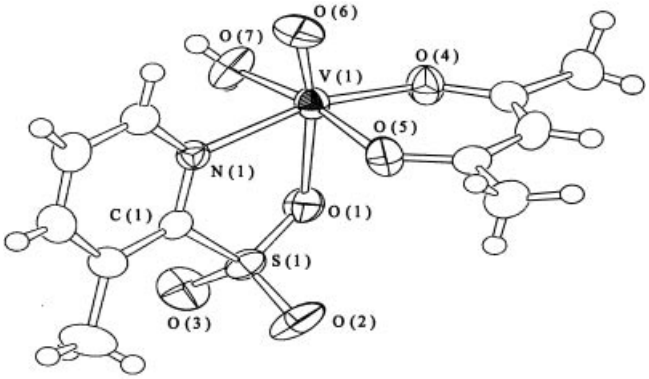

Figure 6. ORTEP drawing of [VO(acac)(3-mpSO$_3$)(H$_2$O)] (**11**)

Hydrogen-bonded Supramolecules

The coordinated water molecules of mononuclear compounds **3**−**11** as well as the lattice water molecule of **10** are engaged in the formation of intermolecular hydrogen bonds between the mononuclear units leading to the construction

Table 3. Crystal data for compounds **1**−**11**

Compound	**1**	**2**	**3**	**4**
T/K	296	296	296	296
Empirical formula	$C_{12}H_{12}CuN_2O_6S_2$	$C_{12}H_{12}N_2O_6S_2Zn$	$C_{12}H_{16}MnN_2O_8S_2$	$C_{12}H_{16}FeN_2O_8S_2$
M_r	407.90	409.74	435.32	436.23
Crystal system	monoclinic	monoclinic	monoclinic	monoclinic
Space group	$P2_1/n$(No. 14)	$P2_1/c$(No. 14)	$C2/c$(No. 15)	$C2/c$(No. 15)
a (Å)	18.627(2)	4.993(1)	19.152(4)	19.069(2)
b (Å)	7.890(2)	14.691(1)	7.472(4)	7.427(2)
c (Å)	4.960(2)	10.194(1)	14.303(4)	14.224(2)
β [°]	89.96(2)	102.40(1)	125.709(10)	125.757(4)
V (Å^3)	729.0(4)	730.4(2)	1661.9(9)	1634.8(4)
Z	2	2	4	4
$D_{calcd.}$ [g cm^{-3}]	1.858	1.863	1.740	1.772
μ [mm^{-1}]	1.817	2.00	1.090	1.223
F(000)	414.00	416.00	892.00	896.00
Data collected	2310	2430	2677	2637
Unique data(R_{int})	2253(0.021)	2209(0.016)	2603(0.015)	2566(0.021)
Observed data [$I > 3\sigma(I)$]	1726	1920	1999	1979
Final *R* [$I > 3\sigma$(I)]	0.124	0.024	0.040	0.036
wR	0.192	0.039	0.053	0.053
Goodness of fit, *S*	5.29	1.55	1.71	1.76
$\Delta\rho_{min.}$, $\Delta\rho_{max.}$ [e·Å^{-3}]	−2.98, 3.36	−0.58, 0.30	−0.69, 0.40	−0.55, 0.36

Compound	**5**	**6**	**7**	**8**
T/K	296	296	296	296
Empirical formula	$C_{12}H_{16}CoN_2O_8S_2$	$C_{12}H_{16}N_2O_8S_2Zn$	$C_{12}H_{16}N_2O_8S_2Zn$	$C_{10}H_{12}N_2O_8S_2Zn$
M_r	439.32	445.77	445.77	417.71
Crystal system	monoclinic	monoclinic	monoclinic	monoclinic
Space group	$C2/c$(No. 15)	$C2/c$(No. 15)	$C2/c$(No. 15)	$C2/c$(No. 15)
a (Å)	19.091(2)	19.058(1)	13.884(2)	13.714(3)
b (Å)	7.367(4)	7.381(1)	7.336(1)	7.150(3)
c (Å)	14.313(2)	14.321(1)	17.932(2)	15.985(3)
β [°]	126.063(6)	126.176(4)	114.065(7)	107.16(1)
V (Å^3)	1627.4(6)	1626.2(3)	1667.7(4)	1497.6(7)
Z	4	4	4	4
$D_{calcd.}$ [g cm^{-3}]	1.793	1.821	1.775	1.852
μ [mm^{-1}]	1.357	1.813	1.768	1.962
F(000)	900.00	912.00	912.00	848.00
Data collected	2636	2630	2714	2433
Unique data(R_{int})	2564(0.021)	2556(0.021)	2612(0.015)	2341(0.016)
Observed data [$I > 3\sigma(I)$]	1776	2056	2274	1746
Final *R* [$I > 3\sigma(I)$]	0.033	0.027	0.033	0.046
wR	0.043	0.038	0.054	0.065
Goodness of fit, *S*	1.25	1.34	1.34	2.19
$\Delta\rho_{min.}$, $\Delta\rho_{max.}$ [e·Å^{-3}]	−0.48, 0.35	−0.47, 0.30	−1.13, 0.35	−1.42, 0.44

Compound	**9**	**10**	**11**
T/K	296	296	296
Empirical formula	$C_{12}H_{16}CoN_2O_8S_2$	$C_{12}H_{18}N_2NiO_9S_2$	$C_{11}H_{15}NO_7SV$
M_r	439.32	457.10	356.24
Crystal system	triclinic	monoclinic	monoclinic
Space group	$P\bar{1}$(No. 2)	$C2/c$(No. 15)	$P2_1/c$(No. 14)
a (Å)	7.430(2)	18.711(3)	13.759(2)
b (Å)	8.507(2)	8.364(2)	7.114(1)
c (Å)	7.207(1)	13.943(2)	15.503(1)
α [°]	99.01(2)		
β [°]	95.35(2)	124.851(8)	103.660(8)
γ [°]	69.45(1)		
V (Å^3)	420.9(1)	1790.7(6)	1474.6(3)
Z	1	4	4
$D_{calcd.}$ [g cm^{-3}]	1.733	1.695	1.605
μ [mm^{-1}]	1.312	1.366	0.844
F(000)	225.00	944.00	732.00
Data collected	5276	2843	4796
Unique data(R_{int})	2456(0.040)	2766(0.031)	4622(0.022)
Observed data [$I > 3\sigma(I)$]	2131	1929	2899
Final *R* [$I > 3\sigma(I)$]	0.034	0.040	0.034
wR	0.048	0.048	0.044
Goodness of fit, *S*	1.72	1.45	1.38
$\Delta\rho_{min.}$, $\Delta\rho_{max.}$ [e·Å^{-3}]	−0.48, 0.31	−1.15, 0.47	−0.35, 0.26

of the two-dimensional (**3**−**10**) and one-dimensional (**11**) supramolecules. Compounds **3**−**8** and **10** showed additional noncovalent π−π interactions, not shown by compounds **9** and **11**. The uncoordinated sulfonato oxygen atoms and coordinated water molecules of compounds **3**−**6** containing 3-mpSO_3^- ligands connect each mononuclear

unit via the intermolecular hydrogen bonds, O(2)··· H-O(4) and O(3)··· H−O(4) (Table 1) to form two-dimensional hydrogen-bonded networks parallel to the *bc* plane. For example, Figure 7 shows the H bonded network of compound **3** parallel to the *bc* plane. In the two-dimensional network, the adjacent molecules along the *b* axis have the same orientation, while the neighboring molecules along the *c* axis have inverted structures of the original molecule and are in the opposite orientation to the original. All of the pyridine rings of the 3-mpSO$_3^-$ ligands are stacked by relatively strong π−π interactions (ca. 3.47Å) as shown for the crystal packing of **3** in Figure 8. Compounds **4**−**6** have the same hydrogen and π−π stacking patterns and their intermolecular parameters are listed in Table 1.

The hydrogen bonding in compound **8** containing the pySO$_3^-$ ligand forms a two-dimensional network parallel to the *ab* plane (Figure 9). The two dimensional hydrogen-bonded sheets are stacked over each other by π−π interactions (ca. 3.70 Å) of the pyridine rings in an offset geometry as shown in Figure 10.

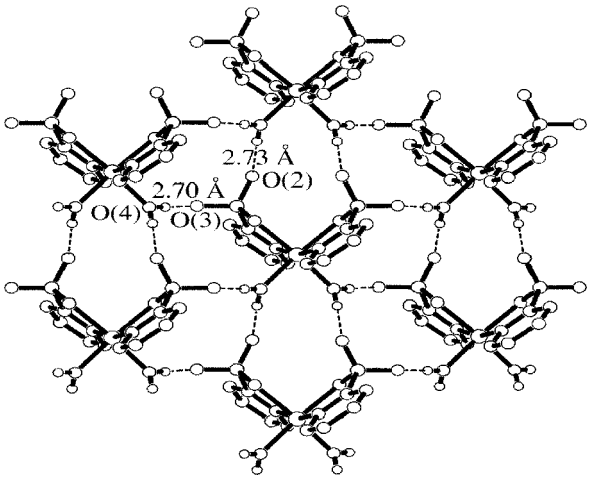

Figure 9. H bonded network of [Zn(PySO$_3$)$_2$(H$_2$O)$_2$] (**8**) parallel to the *ab* plane

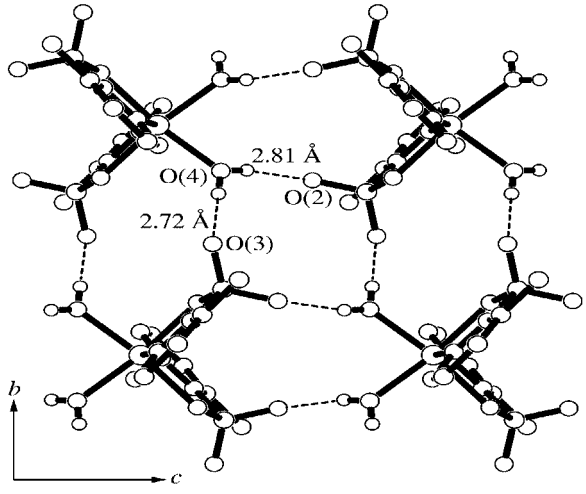

Figure 7. H bonded network of [Mn(3-mpSO$_3$)$_2$(H$_2$O)$_2$] (**3**) parallel to the *bc* plane

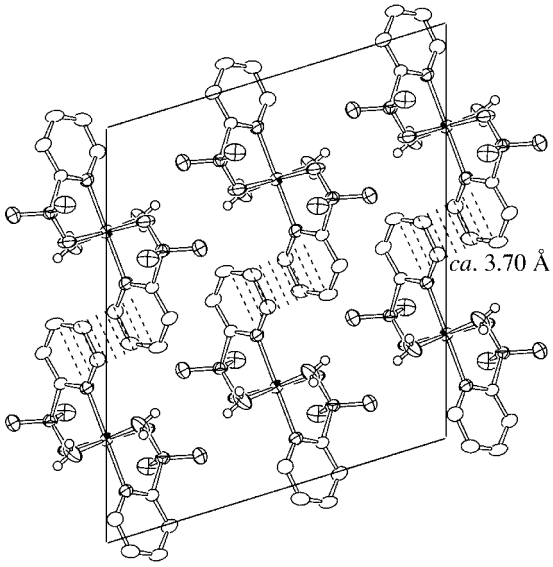

Figure 10. Crystal packing of [Zn(PySO$_3$)$_2$(H$_2$O)$_2$] (**8**) when viewed along the *b* axis

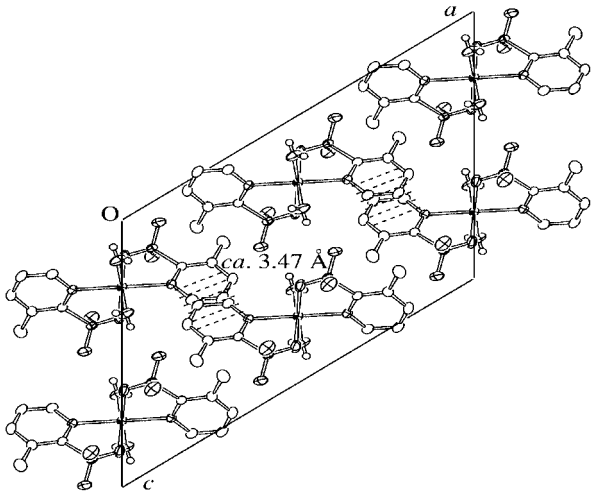

Figure 8. Crystal packing of [Mn(3-mpSO$_3$)$_2$(H$_2$O)$_2$] (**3**) when viewed along the *b* axis

The hydrogen-bonded network of compound **7** containing the 5-mpSO$_3^-$ ligand is also similar to that of **8.** Figure 11 shows that the pyridine rings of the 5-mpSO$_3^-$ ligands are most weakly stacked over each other (ca. 3.96 Å), as compared to the aromatic stacking in the crystals of **3**−**6**, **8** and **10**. Therefore, the calculated density for **7** (1.775 g·cm^{-3}) is clearly less than that for compound **6** (1.821 g·cm^{-3}) even though the two zinc complexes have a common chemical formula. It may be further noted that the

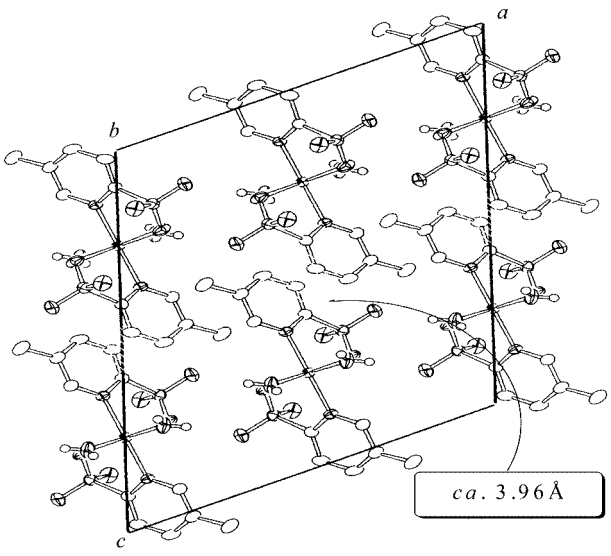

Figure 11. Crystal packing of $[Zn(5\text{-}mpSO_3)_2(H_2O)_2]$ (**7**) when viewed along the *b* axis, geometry as shown in Figure 10

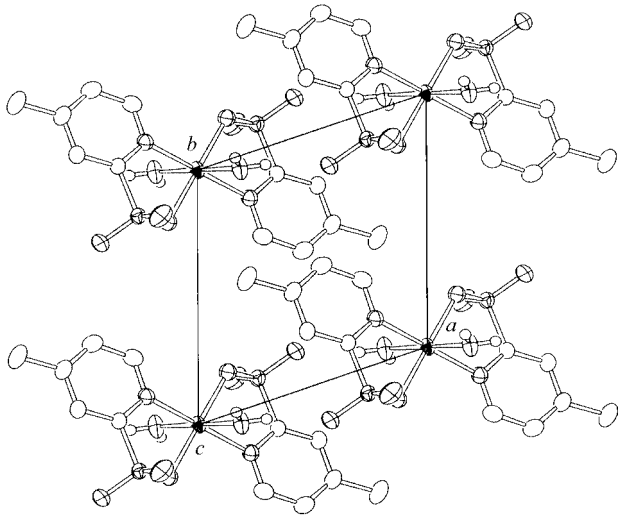

Figure 13. Crystal packing of $[Co(4\text{-}mpSO_3)_2(H_2O)_2]$ (**9**) when viewed along the *c* axis

stacking interaction in compound **6** (ca. 3.50 Å) is stronger than that in compound **8** (above).

It may be interesting to add here that the stoichiometry of zinc(II) complexes **6**−**8** is different from that of **2** which is a one-dimensional polymer as described earlier. The exceptional behavior can be ascribed to the steric effect of the methyl group at the 4-position in the pyridine ring of the 4-$mpSO_3^-$ ligand in **2**. The methyl group sticking out along the Zn(1)-N(1)···C(3) line is probably unfavorable for the formation of hydrogen-bonded networks similar to those of complexes **6**−**8**.

In compound **9**, the hydrogen-bonded network is spread out parallel to the *ac* plane (Figure 12) and it does not show any π−π interaction in the crystal structure (Figure 13) unlike that shown by compound **5**. The methyl group at the 4-position in the 4-$mpSO_3^-$ ligand elongates the structure of **9** along the Co(1)-N(1)···C(3) line and this structural elongation may be the main factor for the absence of π−π interactions in its crystal structure. In compound **10**, two uncoordinated oxygen atoms of 3-$mpSO_3^-$ [O(2), O(3)] participate in intermolecular hydrogen bonds with the coordinated and lattice water molecules leading to the formation of two-dimensional hydrogen-bonded networks (Figure 14). The H bonded sheets are stacked by the π−π interactions of the pyridyl rings in an offset geometry (Figure 15). Finally for compound **11**, the self-assembly of the mononuclear complexes results in the formation of a one-dimensional supramolecular structure along the crystallographic *b* axis (Figure 16).

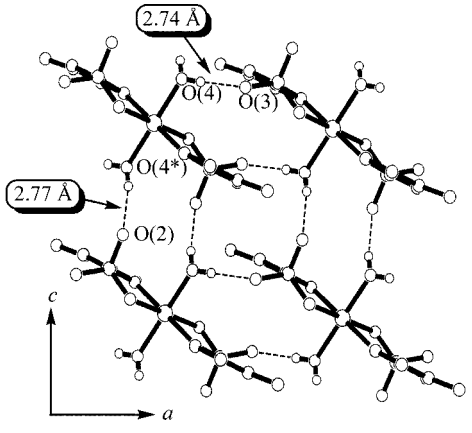

Figure 12. H bonded network of $[Co(4\text{-}mpSO_3)_2(H_2O)_2]$ (**9**) parallel to the *ac* plane

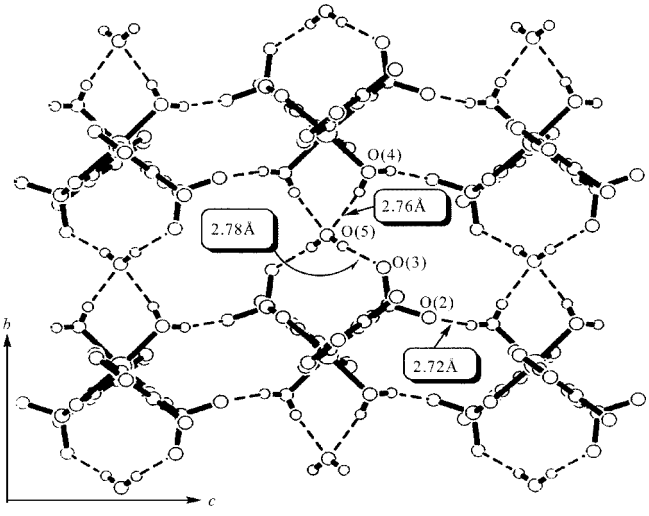

Figure 14. H-bonded network of $[Ni(3\text{-}mpSO_3)_2(H_2O)_2]\cdot H_2O$ (**10**) parallel to the *bc* plane

Magnetic Properties

The magnetic measurement studies of compounds **3** and **11** were carried out in order to check for possible magnetic exchange interactions, if any, between adjacent metal centers of the hydrogen-bonded networks. The variable temperature magnetic susceptibility studies revealed that these compounds are typical paramagnetic compounds with ground spin-states of $S = 5/2$ for **3** and $S = 1/2$ for **11**. The

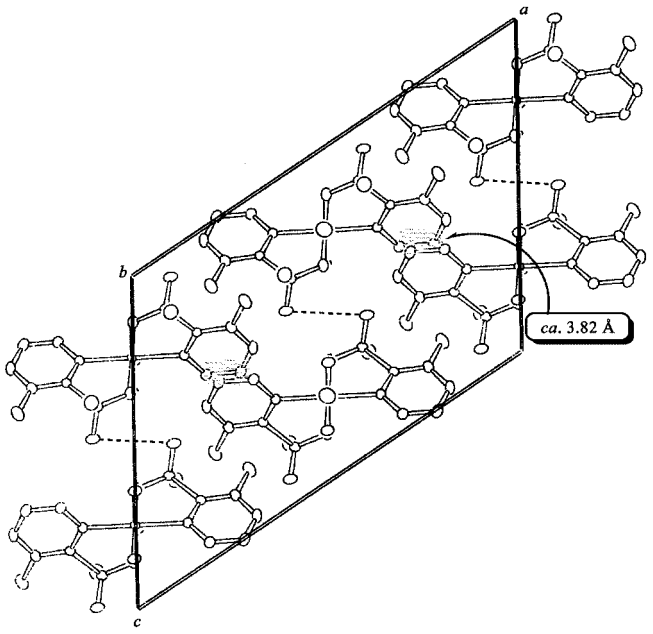

Figure 15. Crystal packing of $[Ni(3\text{-}mpSO_3)_2(H_2O)_2]\cdot H_2O$ (**10**) when viewed along the *b* axis

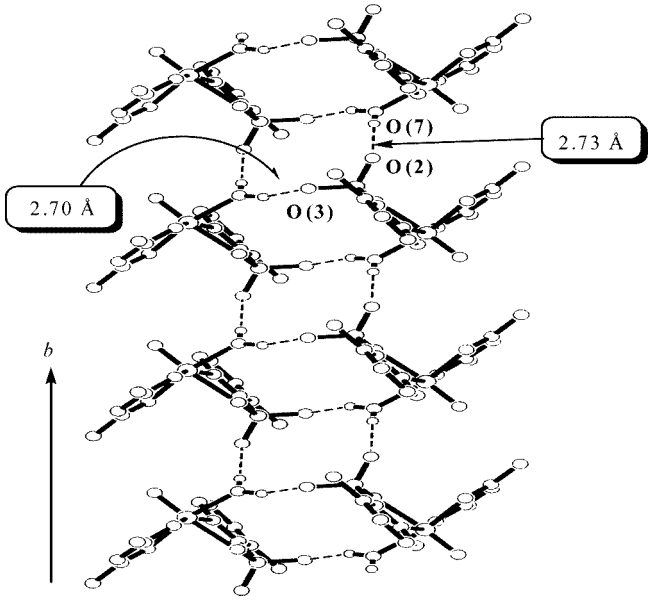

Figure 16. One-dimensional hydrogen-bonded network of complex **11**

magnetic behavior indicates that the intermetallic distances (7.11−7.47 Å) in these network structures are too long to cause any intermolecular magnetic interactions. Other complexes (**1**, **4**, **5**, **9** and **10**) also showed typical paramagnetic behavior.

Solution Phase Behavior

The NMR spectroscopic data of the ligands and zinc(II) complexes recorded in CD_3OD solvent are listed in the Exp. Sect. The ligand spectra are broad as well as partially resolved in view of the exchange of a proton between a N atom and sulfonate SO_3 groups and after the deprotonation of the complexes, the spectra generally become sharp as well as better resolved indicating metal−ligand interaction. Consider first $PySO_3$ and its compound **8**, three pyridyl ring protons show a high-field shift and the magnitude of the shift varies as follows: H(4) > H(5) > H(3). The H(6) proton close to the N coordinating center can be considered as essentially unchanged. The same trend is shown by the compounds **2**, **6** and **7**. The methyl group of $3\text{-}mpSO_3^-$ in compound **6** shows a low-field shift, but the 4-and 5-methyl groups of compounds **2** and **7** show high-field shifts. This difference is understandable in view of the deshielding influence of the sulfonate group, which exerts the largest effect on the methyl group at the 3-position. This is in line with the relatively low up-field shift of H(3) protons of compounds **2**, **7** and **8** which are close to the SO_3 group. NMR spectroscopic studies reveal one very interesting observation that electron density of pyridyl rings is highly polarized and the H(4) (or, 4-Me) and H(5) (or, 5-Me) protons experience high diamagnetic shielding. The NMR spectrum of compound **6** shows that the group $3\text{-}mpSO_3^-$ has distinctly different behavior, which was also reflected in the solid state (compounds **3**−**6**, vide supra).

Conclusions

The location of methyl substituents at the 3-position of the pyridyl ring ($3\text{-}mpSO_3$ ligand) appears to be most suited to induce close π−π stacking interactions (3.47−3.50 Å), a prerequisite for possible electrical conductivity properties. $PySO_3^-$ in compound **8** showed π−π stacking interactions of medium strength (3.70 Å) and the 5-methyl substituent in compound **7** appears to disfavor such interactions leading to a very weak interaction, ca. 3.96 Å. The stacking in $[Ni(3\text{-}mpSO_3)_2(H_2O)_2]\cdot H_2O$ (**10**) is weakened by the presence of water of hydration which increases π−π stacking distance to 3.82 Å compared to other $3\text{-}mpSO_3$ analogs (compounds **3**−**6**). Interestingly the methyl substituent at the 4-position totally disfavors the π−π stacking interactions as for example in compound, $[Co(4\text{-}mpSO_3)_2(H_2O)_2]$ (**9**), because of elongation of the structure along the Co(1)-N(1)···C(3) line. Compound **11** has a columnar one-dimensional structure, which is not suited for such stacking interactions. An analysis of metal−oxygen and metal−nitrogen bond lengths (Table 1) reveals that (i) along the axial side Cu−O bond is weakest, while the Cu−N bonds are shortest and (ii) that water forms very strong metal−oxygen bonds in all the water ligated compounds (**3**−**11**). The longer Cu−O axial bonds are due to Jahn−Teller distortion. Thus copper(II) water ligation appears to be energetically less favored over copper(II) polymer formation as in compound **1**. The factors for the formation of the coordination polymer $[\{Zn(4\text{-}mpSO_3)_2\}_n]$ (**2**), unlike hydrogen-bonded compound of type **9**, are not well understood. However, the compact polymeric structure as in **2** appears energetically more favored.

Experimental Section

Materials and Physical Measurements: All chemicals were purchased from Aldrich, Nacharai Tesque, and Wako Pure Chemical. All reagents and solvents were used without further purification. Infrared spectra in the range 4000−400 cm^{-1} were recorded on KBr discs with a JASCO FTIR 420 spectrophotometer. The ^1H NMR spectra were measured with a JEOL Lambda 400 spectrometer. The magnetic susceptibilities were measured with a Quantum Design SQUID magnetometer MPMS. Elemental analyses were carried out by the Analytical Center of Graduate School of Science in Osaka City University.

Synthesis of Ligands: Pyridine-2-sulfonic acid and its methyl-substituted analogs were prepared by the oxidation of the corresponding pyridine-2-thiones as reported in the literature.[21] The substituted pyridine-2-thiones, namely, 1-H-*x*-methylpyridine-2-thiones (*x* = 3, 4, 5) were synthesized via sulfhydrylation of their corresponding 2-bromopyridines.[22] 1-H-*x*-methylpyridine-2-thione (2.25 g, 0.018mol) was dissolved in 40 mL of glacial acetic acid and then 6.5 mL (0.058 mol) of 30% hydrogen peroxide was added to the mixture. The reaction mixture was heated to 80 °C with stirring until the color of the thione completely disappeared. After removal of the solvent by evaporation under a reduced pressure, the resulting residue was recrystallized from water/methanol (1:1, by volume) to afford colorless crystal of *x*-methylpyridine-2-sulfonic acids.

Caution! *The mixture of acetic acid and hydrogen peroxide produces potentially explosive materials. It is preferable that only limited amounts are prepared at a time, while the temperature is maintained with care. Stirring of the reaction mixture should also be well controlled.*

Pyridine-2-sulfonic Acid ($PySO_3H$): Yield 1.77 g (55%). $C_5H_5NO_3S$ (159.17): calcd. C 37.73, H 3.17, N 8.80; found C 37.72, H 3.09, N 8.77. IR: $\tilde{\nu}$ = ν(N−H) + ν(O−H) 3445 (br. w), 3198 (m), 3132 (s) cm^{-1}; ν(C−H) 3110−2931 (w); δ(N−H) + δ(O−H) 1618 (s); ν(C−N) 1600 (s); ν(C−C) 1520 (s); δ(C−H) 1459 (s), 1417 (w), 1359 (w); ν(S−O) 1303 (s), 1269 (vs), 1247 (vs), 1206 (vs), 1166 (s), 1148 (vs), 1090 (s); ν(C−S) 1041 (vs) cm^{-1}. ^1H NMR (400 MHz, [D_4]methanol, 22 °C): δ = 8.76 (br. s, 1 H, 6-H), 8.69 (t, $J_{H,H}$ = 10.3 Hz, 1 H, 4-H), 8.36 (br. s, 1 H, 5-H), 8.10 (br. s, 1 H, 3-H) ppm.

3-Methylpyridine-2-sulfonic Acid (3-$mpSO_3H$): Yield 1.75 g (50%). $C_6H_7NO_3S$ (173.2): calcd. C 41.61, H 4.07, N 8.09; found C 41.52, H 4.04, N 8.08. IR: $\tilde{\nu}$ = ν(N−H) + ν(O−H) 3210 (m), 3165 (s) cm^{-1}; ν(PyC−H) 3106 (s), 3055 (s); δ(N−H) + δ(O−H) 1614 (m); ν(C−N) 1594 (w); ν(C−C) 1511 (s); δ(C−H) 1459 (m),1446 (m), 1388 (m); ν(S−O) 1316 (m), 1292 (m), 1269 (vs), 1251 (vs), 1237 (s), 1217 (vs), 1210 (sh), 1186 (s), 1158 (s), 1146 (m), 1112 (m); ν(C−S) 1035 (vs); δ(C−CH_3) 816 (m), 802 (m). ^1H NMR (400 MHz, [D_4]methanol, 22 °C): δ = 8.53 (d, $J_{H,H}$ = 6.7 Hz, 2 H, 4-H, 6-H), 7.99 (t, $J_{H,H}$ = 6.7 Hz, 1 H, 5-H); 3.27 (s, 3 H, CH_3) ppm.

4-Methylpyridine-2-sulfonic Acid (4-$mpSO_3H$): Yield 1.93 g (55%). $C_6H_7NO_3S$ (173.2): calcd. C 41.61, H 4.07, N 8.09; found C 41.51, H 4.22, N 8.06. IR: $\tilde{\nu}$ = ν(N−H) + ν(O−H) 3532 (br. vs), 3466 (br. vs), 3363 (m), 3238 (m) cm^{-1}; ν(PyC−H) 3091 (m), 3064 (w); ν(MeC−H) 3008−2858 (w); δ(N−H) + δ(O−H) 1626 (s); ν(C−N) 1602 (m); ν(C−C) 1516 (m); δ(C−H) 1463 (br. s), 1367 (w); ν(S−O) 1297 (m), 1271 (vs), 1245 (vs), 1225 (s), 1200 (m), 1133 (m), 1112 (m); ν(C−S) 1054 (vs); δ(C−CH_3) 836 (vs). ^1H NMR (400 MHz, [D_4]methanol, 22 °C): δ = 8.57 (d, $J_{H,H}$ = 5.9 Hz, 1 H, 6-H), 8.20 (s, 3-H, 1 H), 7.92 (d, $J_{H,H}$ = 5.9 Hz, 1 H, 5-H), 3.24 (s, 3 H, CH_3) ppm.

5-Methylpyridine-2-sulfonic Acid (5-$mpSO_3H$): Yield 1.75 g (50%). $C_6H_7NO_3S$ (173.2): calcd. C 41.61, H 4.07, N 8.09; found C 41.57, H 4.09, N 8.08. IR: $\tilde{\nu}$ = ν(N−H) + ν(O−H) 3475 (br. vs), 3417 (br. vs), 3250 (sh), 3175(sh) cm^{-1}; ν(PyC−H) 3101(m); ν(MeC−H) 3000−2800 (w); δ(N−H) + δ(O−H) 1634 (s); ν(C−N) 1620 (m); ν(C−C) 1556 (m); δ(C−H) 1458 (m), 1436 (m); ν(S−O) 1301 (m), 1267 (vs), 1218 (vs), 1153 (s), 1137 (m); ν(C−S) 1048 (vs); δ(C−CH_3) 849 (s). ^1H NMR (400 MHz, [D_4]methanol, 22 °C): δ = 8.60 (s, 1 H, 6-H), 8.52 (d, $J_{H,H}$ = 7.7 Hz, 1 H, 4-H), 8.23 (d, $J_{H,H}$ = 7.7 Hz, 1 H, 3-H); 3.60 (s, CH_3, 3 H) ppm.

Syntheses of Compounds 1−11

[{Cu(3-$mpSO_3$)$_2$}$_n$] (1): A solution of copper(II) bromide (0.20 g, 0.90 mmol) in 3 mL of water was placed at the bottom of an H-shaped cell, and a solution of 3-$mpSO_3H$ (0.31 g, 1.8 mmol) in 3 mL of water was settled at the other bottom of the cell. The bridging part of the cell was slowly immersed with a methanol/water mixture (1:1 by volume), and the cell was kept steady for 2 weeks. Pale blue crystals of **1** were formed at the bridging part of the cell. Yield 0.140 g (38%). $C_{12}H_{12}CuN_2O_6S_2$ (407.90): calcd. C 35.30, H 2.94, N 6.86; found C 35.28, H 2.92, N 6.76. IR: $\tilde{\nu}$ = ν(PyC−H) 3086 (m) cm^{-1}; ν(MeC−H) 3015−2828 (w); ν(C−N) 1589 (m); ν(C−C) 1580 (w); δ(C−H) 1451 (s), 1374 (w); ν(S−O) 1280 (vs), 1208 (m), 1170 (vs), 1147 (vs), 1075 (m); ν(C−S) 1041 (w), 1015 (s); δ(C−CH_3) 847 (m), 813 (s).

[{Zn(4-$mpSO_3$)$_2$}$_n$] (2): An aqueous solution of 4-$mpSO_3H$ (0.14 g, 0.80 mmol) was neutralized with a diluted aqueous sodium hydroxide solution, and the solvent was evaporated to dryness under reduced pressure. The residue was dissolved in 3 mL of water. The resulting solution was mixed with a solution of zinc(II) bromide (0.091 g, 0.40 mmol) in 1 mL of water. The mixture was stirred for 10 minutes. and subsequently allowed to stand for 1 month at room temperature to obtain colorless crystals of **2**. Yield 0.038 g (23%). $C_{12}H_{12}N_2O_6S_2Zn$ (409.74): calcd. C 35.14, H 2.93, N 6.83; found C 35.15, H 2.90, N 6.73. IR: $\tilde{\nu}$ = ν(PyC−H) 3087 (m) cm^{-1}; ν(MeC−H) 2900−3070 (vw); ν(C−N) 1612 (s); ν(C−C) 1551 (w); δ(C−H) 1437 (m), 1401 (m), 1376 (m); ν(S−O) 1285 (sh), 1277 (vs), 1240 (s), 1172 (vs), 1137 (s), 1114 (s); ν(C−S) 1042 (s), 1024 (s) (νC−S); δ(C−CH_3) 849(s).). ^1H NMR (400 MHz, [D_4]methanol, 22 °C)(ppm): δ = 8.52 (br. d, 1 H, 6-H), 7.90 (s, 1 H, 3-H), 7.50 (s, br., 1 H, 5-H), 2.73 (s, 3 H, CH_3) ppm. Compounds **7** and **9** were prepared similarly.

[Mn(3-$mpSO_3$)$_2$(H_2O)$_2$] (3): A solution of manganese(II) acetate (0.10 g, 0.58 mmol) in 2 mL of water was added to a solution of 3-$mpSO_3H$ (0.20 g, 1.2 mmol) in 4 mL of water and the mixture was stirred for 10 minutes. The solution was kept steady for a week to yield colorless crystals of **3**. Yield 0.096 g (38%). $C_{12}H_{16}MnN_2O_8S_2$ (435.32): calcd. C 33.08, H 3.68, N 6.43; found C 33.17, H 3.67, N 6.43. IR: $\tilde{\nu}$ = ν(O−H) 3409 (br. vs), 3352 (br. vs), 3253 (br. s) cm^{-1}; ν(PyC−H) 3090 (w); ν(MeC−H) 3050−2800 (vw); δ(O−H) 1657 (s); ν(C−N) + ν(C−C) 1583 (m); δ(C−H) 1455 (m), 1415 (w), 1392 (w); ν(S−O) 1238 (vs), 1217 (s), 1191 (vs), 1154 (s), 1123 (w), 1076 (m); ν(C−S) 1029 (vs); δ(C−CH_3) 839 (m), 804 (s). Compounds **8** and **10** were prepared similarly.

[Fe(3-$mpSO_3$)$_2$(H_2O)$_2$] (4): A vial containing iron(II) chloride tetrahydrate (0.16 g, 0.80 mmol) was placed under argon to displace the air, and then 2 mL of degassed water was added to the vial to dissolve the salt. A solution of 3-$mpSO_3H$ (0.28 g, 1.6 mmol) in

5 mL of degassed water was added dropwise to the metal-containing solution by a syringe. The mixture was allowed to stand for 2 days, yielding yellow crystals of **4**, stable in air and moisture. Yield 0.069 g (20%). $C_{12}H_{16}FeN_2O_8S_2$ (436.23): calcd. C 33.01, H 3.67, N 6.42; found C 33.04, H 3.68, N 6.46. IR: $\tilde{\nu}$ = ν(O−H) 3417 (br. vs), 3349 (br. vs), 3253 (br. s) cm^{-1}; ν(PyC−H) 3092 (w), 3064 (w); ν(MeC−H) 3020−2881 (w); δ(O−H) 1658 (s); ν(C−N) + ν(C−C) 1581 (m); δ(C−H) 1456 (m), 1416 (w), 1391 (w); ν(S−O) 1238 (vs), 1217 (w), 1194 (s), 1154 (s), 1125 (w), 1076 (m); ν(C−S) 1027 (s); δ(C−CH_3) 840 (m), 804 (s).

[Co(3-mpSO$_3$)$_2$(H$_2$O)$_2$] (5): A solution of cobalt(II) bromide hexahydrate (0.10 g, 0.31 mmol) in 2 mL of water was added to a solution of 3-mpSO$_3$H (0.11 g, 0.62 mmol) in 5 mL of water and the mixture was stirred for 10 minutes. The solution was concentrated slowly to ca. 3 mL in a dessicator under water vapor pressure, yielding reddish purple crystals of **5**. Yield 0.049 g (36%). $C_{12}H_{16}CoN_2O_8S_2$ (439.32): calcd. C 32.78, H 3.64, N 6.37; found C 32.73, H 3.64, N 6.37. IR: $\tilde{\nu}$ = ν(O−H) 3433 (br. vs), 3358 (br. vs), 3260 (br. s) cm^{-1}; ν(PyC−H) 3092 (w), 3065 (w); ν(MeC−H) 3000−2827 (vw); δ(O−H) 1657 (s); ν(C−N) + ν(C−C) 1586 (m); δ(C−H) 1458 (s), 1391 (w); ν(S−O) 1241 (vs), 1219 (m), 1186 (vs), 1152 (s), 1127 (m), 1076 (m); ν(C−S) 1027 (vs);); δ(C−CH_3) 841 (m), 805 (s).

[Zn(3-mpSO$_3$)$_2$(H$_2$O)$_2$] (6): A solution of zinc(II) bromide (0.091 g, 0.40 mmol) in 2 mL of water was added to a solution of 3-mpSO$_3$H (0.14 g, 0.80 mmol) in 5 mL of water, and the mixture was stirred for 10 minutes. The solution was left for two weeks to yield colorless crystals of **6**. Yield 0.040 g (22%). $C_{12}H_{16}N_2O_8S_2Zn$ (445.77): calcd. C 32.30, H 3.59, N 6.28; found C 32.30, H 3.58, N 6.26. IR: $\tilde{\nu}$ = ν(O−H) 3424 (br. vs), 3356 (vs), 3255 (vs) cm^{-1}; ν(PyC−H) 3093 (m), 3066 (m); ν(MeC−H) 3025−2856 (w); δ(O−H) 1655 (s); ν(C−N) 1587 (s); ν(C−C) 1541 (w); δ(C−H) 1454 (s), 1419 (w), 1391 (m); ν(S−O) 1282 (m), 1237 (vs), 1197 (vs), 1157 (vs), 1127 (s), 1078 (s); ν(C−S) 1031 (vs); δ(C−CH_3) 842 (m), 806 (s). ^{1}H NMR (400 MHz, [D$_4$]methanol, 22 °C): δ = 8.60 (d, $J_{H,H}$ = 4.9 Hz, 1 H, 6-H), 7.99 (d, $J_{H,H}$ = 7.7 Hz, 1 H, 4-H); 7.59 (dd, $J_{H,H}$ = 4.9, 7.7 Hz, 1 H, 5-H), 3.41 (s, 3 H, CH_3) ppm.

[Zn(5-mpSO$_3$)$_2$(H$_2$O)$_2$] (7): Yield 0.068 g (34%). $C_{12}H_{16}N_2O_8S_2Zn$ (445.77): calcd. C 32.30, H 3.59, N 6.28; found C 32.43, H 3.58, N 6.20. IR: $\tilde{\nu}$ = ν(O−H) 3359 (vs), 3245 (s) cm^{-1}; ν(PyC−H) + ν(MeC−H) 3100−2900 (vw); δ(O−H) 1649 (s); ν(C−N) 1598(m); ν(C−C) 1577 (w); δ(C−H) 1473 (m), 1378 (m); ν(S−O) 1298 (m), 1233 (vs), 1207 (vs), 1157 (s), 1125 (s); ν(C−S) 1030 (vs); δ(C−CH_3) 835 (s). ^{1}H NMR (400 MHz, [D$_4$]methanol, 22 °C): δ = 8.58 (s, 1 H, 6-H), 8.02 (d, $J_{H,H}$ = 8.2 Hz, 1 H, 4-H), 7.95 (d, $J_{H,H}$ = 8.2 Hz, 1 H, 3-H); 3.05 (s, 3 H, CH_3) ppm.

[Zn(PySO$_3$)$_2$(H$_2$O)$_2$] (8): Yield 0.016 g (31%). $C_{10}H_{12}N_2O_8S_2Zn$ (417.71): calcd. C 28.73, H 2.87, N 6.70; found C 28.84, H 2.82, N 6.70. IR: $\tilde{\nu}$ = ν(O−H) 3335 (br. vs), 3240 (s) cm^{-1}; ν(PyC−H) 3107(m); δ(O−H) 1650 (s); ν(C−N) 1596 (s); ν(C−C) 1568 (w); δ(C−H) 1470 (m), 1436 (s); ν(S−O) 1300 (m), 1235 (vs), 1205 (vs), 1170 (s), 1159 (s), 1101 (m), 1056 (m); ν(C−S) 1032 (vs). ^{1}H NMR (400 MHz, [D$_4$]methanol, 22 °C): δ = 8.72 (d, $J_{H,H}$ = 5.1 Hz, 1 H, 6-H), 8.18 (t, $J_{H,H}$ = 7.8 Hz, 1 H, 4-H), 8.08 (d, $J_{H,H}$ = 7.8 Hz, 1 H, 3-H), 7.69 (t, $J_{H,H}$ = 6.2 Hz, 1 H, 5-H) ppm.

[Co(4-mpSO$_3$)$_2$(H$_2$O)$_2$] (9): Yield 0.130 g (38%). $C_{12}H_{16}CoN_2O_8S_2$ (439.32): calcd. C 32.78, H 3.64, N 6.37; found C 32.94, H 3.64, N 6.42. IR: $\tilde{\nu}$ = ν(O−H) 3375 (br. vs), 3260 (br. s) cm^{-1}; ν(PyC−H) 3081 (m); ν(MeC−H) 2964−2834 (w); δ(O−H) 1654 (s); ν(C−N) 1611 (s); ν(C−C) 1555 (w); δ(C−H) 1473 (m), 1438 (m), 1405 (m), 1376 (m); ν(S−O) 1240 (vs), 1188 (vs), 1141 (s), 1113 (s), 1036 (s); ν(C−S) 1018 (vs); δ(C−CH_3) 847 (s).

[Ni(3-mpSO$_3$)$_2$(H$_2$O)$_2$].H$_2$O (10): Yield 0.12 g (66%). $C_{12}H_{18}N_2NiO_9S_2$ (457.10): calcd. C 31.50, H 3.94, N 6.13; found C 31.78, H 3.90, N 6.23. IR: $\tilde{\nu}$ = ν(O−H) 3453 (br. vs), 3366 (br. vs), 3266 (br. s) cm^{-1}; ν(PyC−H) 3094 (m), 3066 (m); ν(MeC−H) 3000−2800 (vw); δ(O−H) 1655 (s); ν(C−N) + ν(C−C) 1588 (m); δ(C−H) 1457 (s), 1391 (m); ν(S−O) 1243 (vs), 1186 (vs), 1155 (vs), 1077 (s); ν(C−S) 1026 (vs); δ(C−CH_3) 843 (s), 807 (s).

[VO(acac)(3-mpSO$_3$)(H$_2$O)] (11): A solution of bis(acetylacetonato)vanadium(IV) oxide (0.11 g, 0.40 mmol) in 2 mL of methanol was added to a solution of 3-mpSO$_3$H (0.14 g, 0.80 mmol) in 5 mL of water. The navy blue mixture was stirred for 5 minutes and left at room temperature for 2 days to afford navy blue crystals of **11**. Yield 0.098 g (68%). $C_{11}H_{15}NO_7SV$ (356.24): calcd. C 37.05, H 4.24, N 3.93; found C 37.17, H 4.27, N 3.96. IR: $\tilde{\nu}$ = ν(O−H) 3324 (br. vs), 3222 (br. vs) cm^{-1}; ν(PyC−H) 3092 (w); ν(MeC−H) 3001−2884 (w); δ(O−H) 1648 (s); ν(C−N) + ν(C−C) + ν(C−O) 1578 (vs), 1525 (vs); δ(C−H) + ν(CH=C) 1452 (m), 1430 (m), 1366 (vs); ν(S−O) 1284 (s), 1259 (vs), 1192 (vs), 1156 (s), 1077 (m); ν(C−S) 1031 (vs); ν(V−O) 974 (vs); δ(C−CH_3) 841 (m), 811 (s).

X-ray Crystallography: For all crystals intensity data were collected on a Rigaku AFC-7S diffractometer with a graphite-monochromated Mo-K_α radiation (λ = 0.71069 Å) at 296 K using the ω−2θ scan technique to a maximum 2θ value of 60.° Three standard reflections monitored after every 150 reflections were used for the crystal decay corrections. The observed reflections [$I > 3\sigma(I)$] were extracted from the unique reflections, and the data were corrected for Lorentz and polarization effects. An absorption correction was applied using the empirical ψ-scan method. All crystallographic calculations were carried out using teXsan programs.[23] The structure was solved by the direct methods (SIR92),[24] and refined with full-matrix least-squares techniques,[25] with anisotropic displacement parameters for the non-hydrogen atoms. Some hydrogen atoms were located on difference Fourier maps and refined isotropically, the rest were located in calculated positions and included in the refinement. Table 3 contains crystal data for complexes **1**−**11**. CCDC-205227 to -205236 for complexes **1**−**5**, **7**−**11**, respectively, and -116650 for complex **6** contain the supplementary crystallographic data for this paper. These data can be obtained free of charge at www.ccdc.cam.ac.uk/conts/retrieving.html [or from the Cambridge Crystallographic Data Centre, 12 Union Road, Cambridge CB2 1EZ, UK; Fax: (internat.) + 44-1223-336-033; E-mail: deposit@ccdc.cam.ac.uk]

Acknowledgments

T. S. L. thanks the Japan Society for Promotion of Science for Invitation Fellowship. He also thanks the Guru Nanak Dev University, Amritsar, India for leave. Financial assistance from Ministry of Education, Science and Culture, Japan. Elemental analysis services rendered by the Analytical Center of Osaka City University are gratefully acknowledged. The authors are grateful to the referees for useful comments.

[1] J. M. Lehn, *Supramolecular Chemistry: Concepts and Perspectives*; Wiley-VCH, Weinheim, **1995**, p. 89 and 139.
[2] G. R. Desiraju, *Angew. Chem. Int. Ed. Engl.* **1995**, *34*, 2311−2327.
[3] V. Baron, B. Gillon, A. Cousson, C. Mathoniere, O. Kahn, A. Grand, L. Ohrstrom, B. Delley, M. Bonnet, J. X. Boucherle, *J. Am. Chem. Soc.* **1997**, *119*, 3500−3506.

[4] M. Munakata, L. P. Wu, T. K. Sowa, *Adv. Inorg. Chem.* **1999**, *46*, 173−303.
[5] H. Zhang, X. Wang, B. K. Teo, *Coord. Chem. Rev.* **1999**, *183*, 157−195.
[6] R. Cortes, L. Lezama, J. L. Pizarro, M. I. Arriortua, T. Rojo, *Angew. Chem. Int. Ed. Engl.* **1996**, *35*, 1810−1812.
[7] H. Kobayashi, H. Tomita, T. Naito, A. Kobayashi, F. Sakai, T. Watanabe, P. Cassoux, *J. Am. Chem. Soc.* **1996**, *118*, 368−377.
[8] S. Kitagawa, M. Kondo, *Bull. Chem. Soc. Jpn.* **1998**, *71*, 1739−1753.
[9] E. S. Raper, *Coord. Chem. Rev.* **1997**, *165*, 475−567 (and refs. therein).
[10] K. Kitano, R. Tanaka, T. Kimura, T. Tsuda, S. Shimizu, H. Takagi, T. Nishioka, D. Shiomi, A. Ichimura, I. Kinoshita, K. Isobe, S. Ooi, *J. Chem. Soc., Dalton Trans.* **2000**, 995−1000 (and refs. therein).
[11] T. S. Lobana, A. Castineiras, *Polyhedron* **2002**, *21*, 1603−1611.
[12] W. Su, M. Hong, J. Weng, Y. Liang, Y. Zhao, R. Cao, Z. Zhou, A. S. C. Chan, *Inorg. Chim. Acta* **2002**, *331*, 8−15 (and refs. therein).
[13] M. Hong, Y. Zhao, W. Su, R. Cao, M. Fujita, Z. Zhou, A. S. C. Chan, *Angew. Chem. Int. Ed.* **2000**, *39*, 2468−2470.
[14] T. S. Lobana, S. Paul, A. Castineiras, *J. Chem. Soc., Dalton Trans.* **1999**, 1819−1824.
[15] F. Charbonnier, R. Faure, H. Loiseleur, *Cryst. Struct. Commun.* **1981**, *10*, 1129−1132.
[16] M. Murata, M. Kojima, A. Hioki, M. Miyagawa, M. Hirotsu, K. Nakajima, M. Kita, S. Kashino, Y. Yoshikawa, *Coord. Chem. Rev.* **1998**, *174*, 109−131.
[17] K. Kimura, T. Kimura, I. Kinoshita, N. Nakashima, K. Kitano, T. Nishioka, K. Isobe, *Chem. Commun.* **1999**, 497−498.
[18] K. Umakoshi, T. Yamasaki, A. Fukuoka, H. Kawano, M. Ichikawa, M. Onishi, *Inorg. Chem.* **2002**, *41*, 4093−4095.
[19] E. M. Barranco, O. Crespo, M. C. Giemno, P. G. Jones, A. Laguna, C. Sarroca, *J. Chem. Soc., Dalton Trans.* **2001**, 2523−2529.
[20] (Eds.: J. E. Huheey, E. A. Keiter, R. L. Keiter), *Inorganic Chemistry: Principles of Structure and Reactivity*, 4th Ed., Harper Collins College Publishers, New York, **1993**.
[21] A. M. Comrie, J. B. Stenlake, *J. Chem. Soc.* **1958**, 1853−1854.
[22] E. C. Horning, *Organic Synthesis*, John Wiley & Sons, Inc., New York, **1955**, vol. 3, p. 136−139.
[23] teXsan, *Crystal Structure Analysis Package, Molecular Structure Corporation*, **1985** and **1999**.
[24] A. Altomare, G. Cascarano, C. Giacovazzo, A. Guagliardi, M. C. Burla, G. Polidori, M. Camalli, *J. Appl. Cryst.* **1994**, *27*, 435−436.
[25] G. M. Sheldrick, *SHELXL-97. Program for the Refinement of Crystal Structures.* University of Göttingen, Germany, **1997**.

Received April 30, 2003
Early View Article
Published Online December 4, 2003

